The use of near-infrared and mid-infrared spectroscopy to rapidly measure the nutrient composition and the *in vitro* rumen dry matter digestibility of brown seaweeds

Mairead Campbell, Jordi Ortuño, Anastasios Koidis, and Katerina Theodoridou*

Institute for Global Food Security, Queen's University Belfast, Belfast BT9 5DL, Northern Ireland, UK

*Corresponding author: Katerina Theodoridou. Queen's University Belfast, 19 Chlorine Gardens, BT9 5DL Belfast, Northern Ireland, UK. Phone: +44 (0) 2890974585. E-mail: k.theodoridou@qub.ac.uk

Abstract

Brown seaweeds are the most studied and exploited algae type for ruminant nutrition due to their biomass availability, ease of harvest and content of bioactive compounds. Infrared spectroscopy represents a rapid, non-invasive and chemical-free technique that is widely applied for the chemical characterization and digestible quality of many terrestrial forages. However, there is limited information regarding its application to seaweeds. This study compared the effectiveness of Near-Infrared (NIR: 9000-4000 cm^{-1}) and Mid-Infrared (MIR: 4000-400 cm^{-1}) spectroscopy to measure the nutritional value and *in vitro* dry matter rumen digestibility of brown seaweeds. Due to the small number of seaweed samples available, 40 samples were analysed in triplicate with a total dataset of 120 samples. For partial least-squares regression model development and evaluation purposes, the dataset (n = 120) was divided into two subsets, the first one for training and model development purposes (70% of data, n = 84), and the second one for model testing and evaluation (internal evaluation) purposes (30% of data, n = 36).Partial least-squares regression was employed to develop multivariate calibration models which were internally and externally validated. The samples were analysed using established wet chemistry methods which were regarded as the reference methods. NIR showed high accuracy for the quantitative prediction of crude protein (R^2P = 0.99; RMSEP = 0.51; RER = 26.9; RPD = 6.9) and total polyphenolic content (R^2P = 0.94; RMSEP = 0.20; RER= 10; RPD= 3.2), whereas MIR could only accurately predict crude protein (R^2P = 0.96; RMSEP = 1.12; RER = 11.64; RPD = 3.14). Ash, neutral and acid detergent fibre, lignin (sa) and *in vitro* dry matter rumen digestibility models showed limited applicability for quantitative measurements (R^2P < 0.85; RPD <

2). Overall, NIR and MIR could be used to rapidly evaluate the nutritional composition and digestibility of brown seaweeds in their dried form but further evaluation on an external database would be required to assess the robustness of these models on unrelated data. Furthermore, the use of these spectroscopic methods showed lower accuracy and precision compared to wet chemistry methods, which better qualifies them for screening rather than confirmatory analysis.

Keywords: Brown Seaweed, Ruminant feed; In vitro; Near-Infrared; Mid-Infrared; Spectroscopy; Chemometrics

Abbreviations: NIR: Near-Infrared spectroscopy; MIR: Mid-Infrared spectroscopy; SD: standard deviation; Min: minimum; Max: maximum; SE: Standard Error; TPC: total polyphenolic content; CP: crude protein; aNDF: neutral detergent fibre assayed with a heat stable amylase and expressed inclusive of residual ash; ADF: Acid Detergent Fibre; Lignin (sa): Lignin determined by solubilization of cellulose with sulphuric acid; IVTDMD: *in vitro* true dry matter digestibility; LV: Latent Variables; RMSEC: root mean square error of calibration; R^2C: coefficients of calibration; RMSEP: root mean square error of prediction; R^2P: coefficients of prediction; RMSECV: root mean square error of cross-calibration; RER: Range Error Ratio; RPD: Residual Predictive Performance; SEL: Standard Error of reference method

1. Introduction

Brown seaweeds are ubiquitous to the temperate waters of North-Western Europe, where coastal farming communities have traditionally used them as a valuable feed resource for cattle, horse and sheep for centuries (Evans and Critchley, 2014). In recent years, research has sparked renewed interest in the value of feeding seaweed to ruminant livestock which is underpinned by their unique chemical profile (Maia et al., 2019). Seaweeds are rich in complex carbohydrates and organic minerals and contain an array of bioactive metabolites, including polyphenolic compounds, which have demonstrated various antimicrobial, anti-inflammatory and antioxidant properties (Holdt and Kraan, 2011). Previous authors have discussed the advantages of feeding seaweeds as a functional feed source to improve animal health as an immunostimulant (Wang and McAllister, 2011), and to reduce ruminal methane emissions (Bikker et al., 2020; Molina-Alcaide et al., 2017).

Understanding the chemical profile of seaweeds is key to recognising their value as a feed ingredient. Recent studies revealed the chemical composition of seaweeds using established wet chemistry methods (Bikker et al., 2020; Maia et al., 2019; Molina-Alcaide et al., 2017). These methods provide reliable measurements of various chemical parameters used in diet formulations, but the requirements for skilled technicians, laborious protocols and destructive sampling techniques limit their use for routine feed analysis. Furthermore, *in vitro* models, which are widely used as a screening tool to determine the digestibility of different feeds, require the use of digesta from rumen cannulated animals to replicate rumen conditions in the laboratory. These requirements exacerbate the cost of resources necessary for accurate and reliable feed analysis (Yáñez-Ruiz et al., 2016). Infrared spectroscopy can provide a more rapid, non-invasive and chemical-free technique for animal feed analysis (Manley, 2014). Once calibrations are developed, spectroscopic techniques are easy to use and offer a more cost and time-effective decision-making tool for farmers and livestock nutritionists when formulating diets. Furthermore, given the wide variability in the chemical composition of seaweeds, the potential to use portable, handheld infrared technologies, such as

those currently used in food and feed production (Ellis et al., 2015; Haughey et al., 2015), would provide a rapid, point-of-source evaluation tool.

The analysis of feeds by infrared spectroscopy combines rapid vibrational spectroscopic techniques with mathematical modelling to provide chemo-structural information on feed components. However, few studies have applied these techniques to seaweeds. Near-Infrared (NIR) and Mid-Infrared (MIR) spectroscopy provide information on the feed molecular constructs, which are directly related to the nutritional composition (Bai et al., 2016). For decades, NIR has been an invaluable tool in animal feed analysis to determine the chemical composition of a range of feeds including forages, grains, by-products and silages (Foskolos et al., 2015; McDonald et al., 2011). The NIR portion of the electromagnetic spectrum provides structural information on overtones and combination bands representative of C–H, N–H, O–H and C=O bonds of feed constituents (e.g. proteins and carbohydrates) (Manley, 2014). Less is known about the application of the MIR region for feed analysis; however, the development of Fourier-transform MIR spectrometers combined with attenuated total reflectance has facilitated research on the application of MIR for a range of purposes, including animal feed analysis (Theodoridou and Yu, 2013). Concerning seaweeds, MIR spectroscopy was previously utilised to examine their polysaccharide content (Gómez-Ordóñez and Rupérez, 2011; Pereira et al., 2013; Sakugawa et al., 2004), whilst studies on the use of MIR to describe the nutritive value of ruminant feeds are few and limited to terrestrial plants and animal by-products (Bai et al., 2016; Belanche et al., 2014, 2013; Shi et al., 2019). Considering the rapidly growing interest in the use of seaweed as a feed ingredient in ruminant diets, the aim of this study was to investigate the use of IR spectroscopy coupled with chemometric modelling to evaluate the nutritive value and rumen digestibility of brown seaweeds. Furthermore, it is currently unknown whether MIR spectroscopy can predict feed composition with a greater accuracy than is achieved with NIR spectroscopy (Belanche et al., 2014), thus, another objective of the study was to compare the application of MIR and NIR as a novel tool for seaweed feed analysis.

2 Material and methods

2.1 Seaweed sampling

The seaweeds (n=40) were collected over one year (March 2017 to February 2018) in Bangor, County Down, Northern Ireland (54°39'58.6"N 5°39'53.4"W). Four species of brown seaweed, namely *Ascophyllum nodosum* (ASC), *Fucus vesiculosus* (FVS), *Saccharina latissima* (SAC) and *Laminaria digitata* (LAM), were collected from the seashore during low tide. The seaweed species were confirmed by a marine biologist at Queen's University Belfast Marine Laboratory, Portaferry. The seaweeds were washed with cold tap water, cut in <5 cm sections and frozen immediately at -20°C. All samples were then lyophilised using a Christ Alpha 1-4 LD Plus freeze dryer (Christ, Osterode, Germany) and ground using a Polymix PX-MFC 90D mechanical grinder to pass through a 1 mm sieve for further analysis. For spectroscopic analysis, the seaweeds were finely ground using a fit with a 0.5 mm screen.

2.2 Reference method analysis

Ground seaweeds were analysed for residual Dry Matter (DM) (AOAC 930.15; 2000), ash (AOAC 942.05; 2000), Neutral Detergent Fibre (aNDF; 1 hour boiling in neutral detergent (ND) solution, with amylase and sodium sulphite) and Acid Detergent Fibre (ADF; 1 hour boiling in acid detergent solution) as described by Van Soest et al. (1991), and lignin (sa) (3 hours in 72% sulphuric acid solution) (Robertson and Van Soest, 1981). The results of the fibre analysis were expressed inclusive of residual ash. Nitrogen (N) content was analysed using Leco Protein/N Analyser (FP-528, Leco Corp., St Joseph, MI, USA) and crude protein (CP) was calculated using N x 5.0, as suggested by Angell et al. (2016). Total Polyphenolic Content (TPC) was determined using the Folin–Ciocalteu (FC) method, adapted from Li et al. (2017). Briefly, seaweed samples were extracted using 0.2 ± 0.05 g of lyophilised seaweed in an acetone-water mix (70:30; solid to liquid ratio 1:20). The mixture was ultra-sonicated in a water bath (VWR, Model USC600TH) for 30 mins at 20°C and centrifuged for 2 mins at 2200 x *g* (Sorvall Legend RT, Germany). Following the addition of Folin- Ciocalteu (1N)

reagent and aqueous sodium carbonate (20% w/v), the solution was stored in the dark for 60 mins in transparent cuvettes, and the absorbance was read at 725 nm (Jenway 6305, Barloworld Scientific Ltd., Dunmow, Essex, UK). Phloroglucinol (Sigma-Aldrich, Dorset, UK) was used as an external standard (1.0 to 50 µg/ml), and results were expressed as g phloroglucinol equivalents per kg DM (g PGE/kg DM). All chemical analyses were carried out in triplicate and reported as % DM.

In vitro dry matter digestibility was determined using the Daisy^{II} incubation method followed by aNDF digestion in an ANKOM 200 Fibre Analyzer (Ankom Technology Corp., Macedon, NY), as described previously (Holden, 1999). Rumen contents were collected from three post-slaughter bovine rumens from an abattoir in Northern Ireland. The rumen contents were then isothermally transported to the laboratory, filtered through four layers of cheesecloth, mixed and purged with CO_2. The rumen fluid was added to the digestion jar containing the pre-warmed (39°C) buffer solution (v/v 1:5). After a 48-hour incubation period, the bags were rinsed four times with distilled water, and the residues were added in a neutral detergent solution, for 60 mins, to remove rumen microbial debris and determine the true dry matter digestibility. The residues were subsequently dried in a convection oven at 60˚C for 48 hours. The *in vitro* true dry matter digestibility (IVTDMD) was calculated as the difference between the dry matter incubated and the residue after neutral detergent treatment divided by the dry matter incubated. A total of two *in vitro* incubation runs were carried out, and each sample was incubated in triplicate.

2.3 Spectral acquisition

The samples were analysed at room temperature using the Antaris II FT-NIR (Thermo Fisher Scientific, Dublin, Ireland). Approximately 10 g of lyophilised seaweed sample was poured into the sample cup (3.2 x 1.5 cm) and analysed at a resolution of 8 cm^{-1}. The samples were scanned 32 times, following a background scan. Three replicates were individually prepared and scanned per sample. After collection, OMNIC 7.2 software (Spectra Tech, Madison, WI, USA) was used to process the data.

Attenuated Total Reflectance-Fourier-Transformed Mid-Infrared vibration spectroscopy (MIR) was performed using a Thermo Nicolet iS5 Spectrometer (Thermo Fisher Scientific, Dublin, Ireland). A small amount (<0.1 g) of lyophilised seaweed was placed on the diamond crystal sample area; equal pressure was applied by the slip clutch pressure tower to ensure the sample completely covered the sample area. Prior to each scanning, the spectra were corrected by subtracting background scans of the clean diamond crystal. The spectral data were obtained using 32 scans per run, at room temperature and a spectral resolution of 4 cm^{-1}. Each sample was analysed in triplicate and the results were processed using the OMNIC 7.2 software.

2.4 Multivariate Model Development

Various spectral pre-processing techniques including Standard Normal Variate (SNV), Derivatisation and Savitzky–Golay smoothing were applied individually and in combination. Mean centering was applied to all data before calibration. This technique subtracts the average values from each variable and can be used to enhance spectral response (Ferreira et al., 2014; Manley, 2014). SNV is commonly applied to reduce light scattering whilst derivatisation can reduce problems associated with overlapping peaks and thereby help extract information on subtle spectral characteristics. Pre-processing treatments were optimised for each chemical parameter. The goodness of model fit was assessed based on maximising coefficients of determination (R^2), which describe the percentage of variability in the chemical components as explained by the regression equation, and minimising root mean standard errors (RMSE).

Principal component analysis (PCA) is an unsupervised multivariate technique used to convert X variables (absorbance values) into new orthogonal variables (principal components) thus eliminating collinearity, or redundant information (Martens and Naes, 1989). PCA was used to identify underlying compositional differences between the samples, examine sample clustering and to identify potential spectral outliers in the dataset. PCA analysis was performed using SIMCA 15.0.2 (Sartorius Stedim Biotech, Göttingen, Germany). Hotelling's T-test was used to calculate the H distances between sample spectra with respect to the mean spectrum; H distances > 3 were

categorised as atypical spectra (Shenk and Westerhaus, 1991) and possible reasons for the sample to be an outlier were explored prior to possible elimination.

Partial least squares regression (PLS-R) is a supervised multivariate method used to establish a linear model which enables the prediction of Y variables from the measured spectrum. In the current study, PLS-R was applied to develop the calibration equations using TQ Analyst software (version 8.3.125; Thermo Fisher Scientific Inc.). The final number of samples selected was 120 and spectra remained unaveraged for the analysis; no outliers were excluded from the datasets since there was no reason to do so from an analytical point of view. The datasets were constructed by assigning each sample a random number using the RANDOM function in MS Excel. The calibration set was composed of 84 samples (70% of total samples) and the remaining 36 samples were used to evaluate the predictive power of the model (validation set). Whole spectrum and targeted wavelength region selection criteria were also applied. Wavelengths relevant to each of the chemical parameters were determined using Regression Coefficient (RC) analysis. This analysis was applied as an objective region selection technique to eliminate information redundancy and identify regions of the infrared spectrum which were sensitive to the prediction of Y variables (de Oliveira et al., 2014). RCs between -0.5 to 0.5 and -0.1 to 0.1, for NIR and MIR, respectively, were used to identify spectral regions correlated to the respective parameter. RC analysis was performed by SIMCA 15.0.2 (Sartorius Stedim Biotech, Göttingen, Germany).

Calibration performance was assessed using cross-validation. The process calculates the optimal number of terms in the regression model by dividing the dataset into cross-validation groups (n= 7) and simulating the algorithm so that all subsets are used once for validation purposes; the optimal number of terms included in the model were chosen to minimise the error and avoid over-fitting the model (Shenk and Westerhaus, 1991). The root mean square error of calibration (RMSEC), the coefficient of determination in calibration (R^2C) and the root mean square error of cross-validation (RMSECV), were calculated to evaluate the predictive ability of the models. The residual predictive deviation (RPD) – defined as the ratio between the standard deviation of the reference population

198 and the RMSECV – and the range error ratio (RER) – defined as the ratio between the range of the
199 validation set and the root mean square error of the prediction set (RMSEP) – were used to assess
200 the accuracy of the models (Fearn, 2002; Williams, 2004). Moreover, the RMSEP and the coefficient
201 of determination in prediction (R^2P) were calculated based on external validation to evaluate model
202 performance. The best regression models were selected by optimising the following combinations:
203 minimise RMSECV and RMSEP, and maximise coefficients of determination, RPD and RER values.
204 Finally, the RMSEP was compared with the laboratory (or reference) error (SEL), as this statistic
205 allows the spectroscopic error to be put in perspective of the error in the reference method (Pojić et
206 al., 2010).

207 **3. Results**

208 **3.1 Reference method analysis**

209 A descriptive summary of the reference method statistics is presented in **Table 1**. The calibration and
210 validation datasets were split at a ratio of 70:30 and showed comparable descriptive statistics for all
211 tested parameters. Therefore, it was considered that randomisation generated an appropriate level
212 of variation, which was representative of the whole dataset.

213 **Table 1.** Descriptive summary of the chemical parameters of brown seaweeds according to the
214 reference methods (%DM, unless stated otherwise).

Descriptor	Ash	TPC	CP	aNDF	ADF	Lignin (sa)	IVTDMD
Mean	21.42	0.74	8.81	36.61	15.4	6.73	0.768
SD	6.15	0.67	3.72	8.53	3.11	3.34	0.157
Min	11.44	0.06	4.31	18.25	8.62	1.11	0.509
Max	37.66	2.14	17.74	53.14	23.63	14.14	0.978
SE	0.73	0.12	0.42	0.92	0.33	0.42	0.017
Mean	23.35	0.62	10.14	37.23	16.13	6.12	0.805
SD	7.56	0.67	4.51	9.41	3.51	3.63	0.150
Min	10.01	0.03	4.25	17.76	9.21	1.31	0.557
Max	38.56	2.15	17.82	54.63	23.84	14.04	0.964

SE	1.30	0.12	0.83	1.62	0.69	0.62	0.025
Mean	21.72	0.65	9.21	36.82	15.60	6.35	0.790
SD	6.53	0.61	4.12	8.31	3.43	3.44	0.155
Min	11.26	0.03	4.10	18.27	8.62	1.14	0.509
Max	37.61	2.14	17.82	51.83	23.81	14.13	0.978
SE	0.77	0.16	0.47	0.95	0.46	0.44	0.018
Mean	22.74	0.73	9.24	36.71	15.90	7.12	0.754
SD	6.84	0.64	3.81	9.81	2.71	3.40	0.156
Min	10.01	0.02	4.12	17.74	9.93	1.14	0.527
Max	38.63	1.77	17.16	54.63	20.82	20.83	0.964
SE	1.19	0.18	0.68	1.69	0.58	0.64	0.027

NIR: Near-Infrared spectroscopy; MIR: Mid-Infrared spectroscopy; SD: Standard Deviation: Min: Minimum; Max: Maximum; SE; Standard Error; TPC: Total Polyphenolic Content; CP: Crude protein; aNDF: Neutral Detergent Fibre; ADF: Acid Detergent Fibre; Lignin (sa): Lignin determined by solubilization of cellulose with sulphuric acid; IVTDMD: *in vitro* True Dry Matter Digestibility.

3.2 Characteristics of NIR and MIR spectra

The NIR and MIR spectral features of the brown seaweeds are shown in **Figure 1**. The bands in the NIR region contain information on the hydrogen-containing organic constituents (e.g. N-H, C-H, O-H) present in the sample. The broad absorption regions were observed in the raw spectra at approximately 8400-8200 cm^{-1}, 6800-6200 cm^{-1}, 5800-5600 cm^{-1}, 5200-5100 cm^{-1} and 5000-4500 cm^{-1}. The typical MIR spectrum (**Figure. 1**) can be divided into two general regions: the functional group region (4000-1800 cm^{-1}) which includes hydroxyl and alkyl stretching behaviours, and the fingerprint region (1500-600 cm^{-1}).

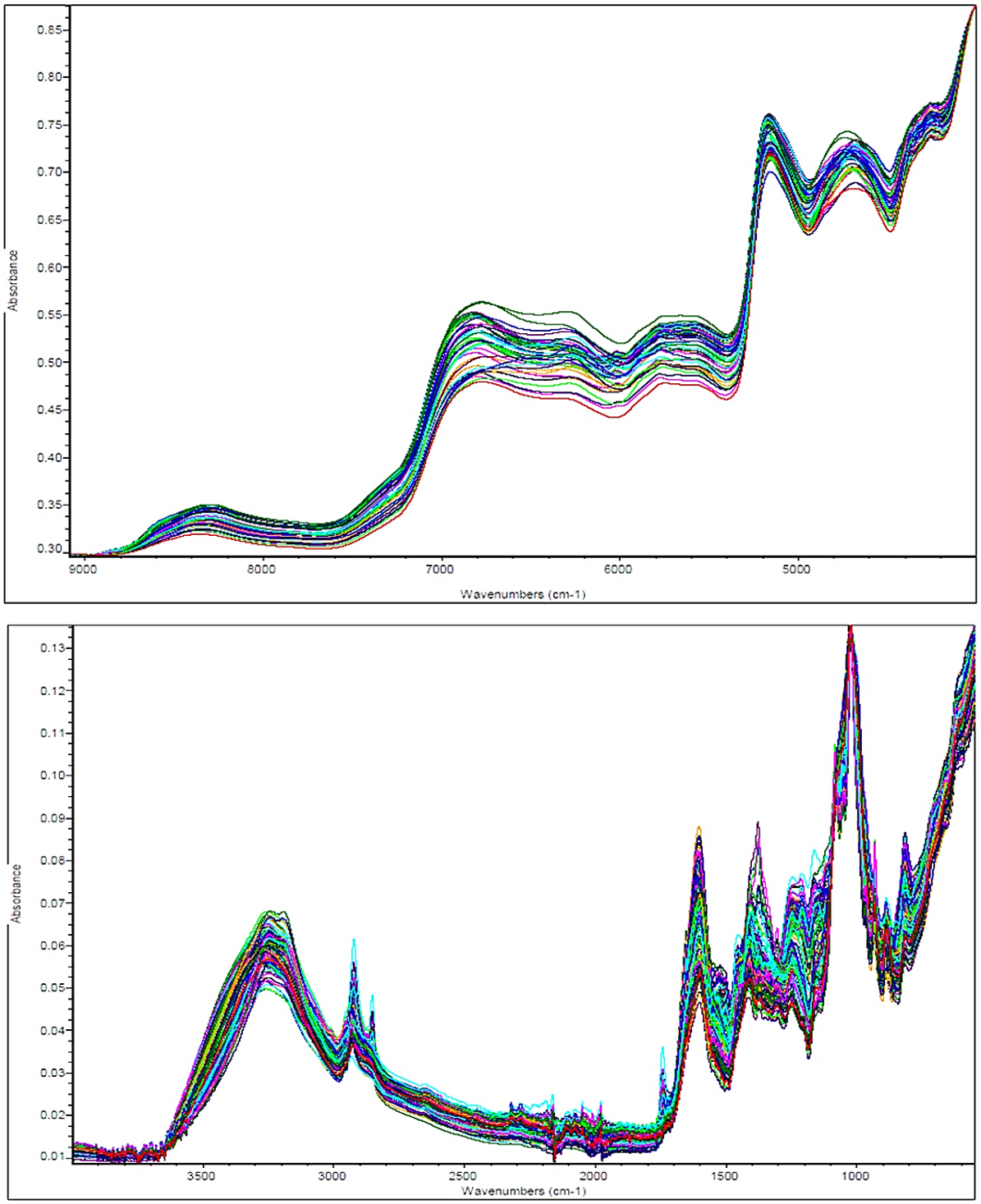

Figure 1. Raw spectra of brown seaweeds (n= 120) obtained by NIR and MIR

Principal Component Analysis (PCA) was used before the application of PLS-R to independently examine the potential clustering of samples and to detect spectral outliers. The PCA results were plotted based on the two highest principal components (PC) scores, as illustrated in **Figure 2**. The first two PCs explained 89 and 6.7% of MIR data variation, respectively. NIR showed better

separations compared to MIR; the first two PCs explained 94 and 4.8% of the variation in the spectral data, respectively. Generally, both techniques achieved separation between *Fucus vesiculosus* (FVS) / *Ascophyllum nodosum* (ASC), and *Saccharina latissima* (SAC) / *Laminaria digitata* (LAM), which reflects taxonomic classifications of the seaweeds: FVS and ASC belong to the order Fucales whilst LAM and SAC are categorised within the order Laminariales.

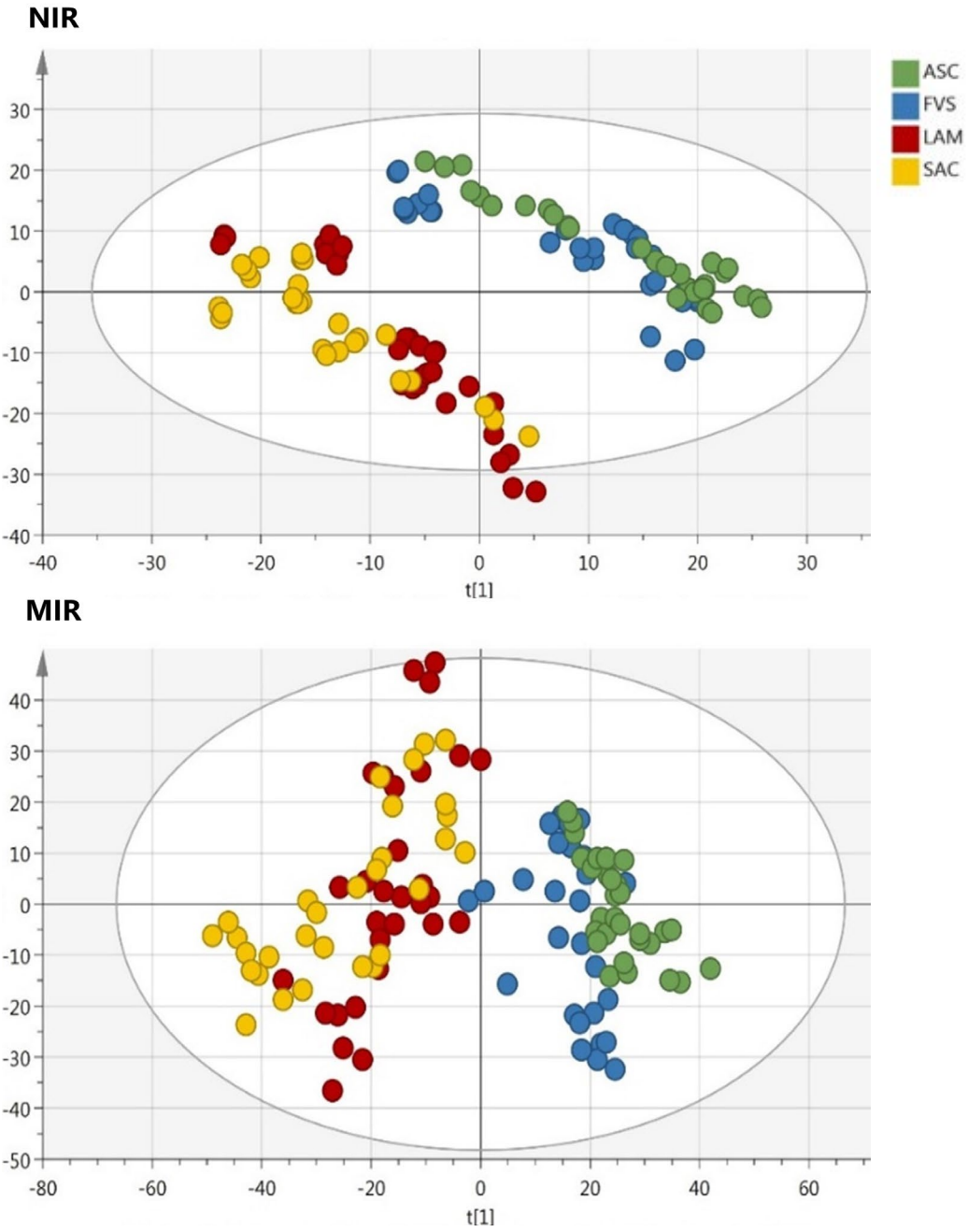

Figure 2. Principal component analysis of NIR and MIR spectral data (n=120) of brown seaweeds (*Ascophyllum nodosum* (ASC); *Fucus vesiculosus* (FVS); *Laminaria digitata* (LAM); *Saccharina latissima* (SAC). Circles represent 95% confidence interval.

3.3 PLS-R model development

Given the small dataset available, the spectra were not averaged before building the PLS-R models. Therefore, smoothing techniques were tested to mitigate spectral noise contributions. Compared to the raw spectra, pre-processing improved model performance for both spectroscopic techniques and all chemical parameters tested (**Supplementary Table S1**). The optimal pre-processing techniques for each parameter were selected based on minimising SE and maximising R^2. Both positive and negative regression coefficient values were obtained, as shown in the RC plots in **Figure 3**. Alongside this, models based on the whole spectrum (i.e. containing the full set of wavenumbers as variables) were developed to compare and optimise the calibration procedure.

There was high sensitivity in the fingerprint region of the MIR spectra (**Figure 3. B1-B5**) for all chemical parameters. Therefore, the fingerprint region was included in all region selection criteria used in MIR regression model development. High RC values were obtained for CP in the MIR regions of 1700-1400 and 3800-3300 cm^{-1} (**Figure 3. B3**), the former of which included the protein region (1620-1550 cm^{-1}). Compared to the use of the whole spectra, region selection did not improve CP models, but notably reduced R^2P from 0.97 to 0.92, respectively, and increased RMSEP from 0.99 to 1.59. NIR spectroscopy showed an excellent CP predictive ability, with an RER > 25 and RPD ≥ 7. As expected, the RC plot (**Figure 3. A3**) showed high sensitivity in the protein band, 5000 - 4500 cm^{-1}, corresponding to N-H and C=O stretching although region selection did not have an impact on model outputs (**Table 2**).

Table 2. The output parameters of the PLS-R models to evaluate the nutritive value and in *vitro* true dry matter rumen digestibility of brown seaweeds.

	NIR/MIR	LV	RMSEC	R^2 C	RMSEP	R^2 P	RMSECV	RER	RPD	SEL
Ash	NIR	5	4.36	0.79	5.03	0.79	5.08	5.69	1.47	0.61
	MIR	4	4.83	0.79	4.18	0.82	5.65	6.84	1.20	
TPC	NIR	9	0.15	0.96	0.20	0.94	0.21	10.14	3.19	0.06
	MIR	6	0.19	0.95	0.23	0.92	0.31	7.54	2.08	
CP	NIR	10	0.43	0.99	0.51	0.99	0.65	26.93	6.92	0.36
	MIR	6	1.10	0.96	1.12	0.96	1.27	11.64	3.14	
aNDF	NIR	9	2.55	0.95	5.58	0.81	6.50	6.61	1.44	0.78
	MIR	8	3.08	0.93	7.01	0.72	7.07	5.26	1.39	
ADF	NIR	7	1.07	0.93	1.87	0.85	2.20	7.80	1.58	0.29
	MIR	9	1.04	0.95	2.29	0.64	2.25	4.76	1.20	
Lignin (sa)	NIR	5	1.46	0.89	1.90	0.85	1.89	6.78	1.90	0.31
	MIR	8	2.12	0.78	2.06	0.81	2.47	9.27	1.38	
IVTDMD	NIR	4	8.65	0.87	11.70	0.81	9.68	3.47	1.54	1.43
	MIR	7	9.06	0.86	13.60	0.72	10.60	3.21	1.47	

LV, Latent Variables; RMSEC, root mean square error of calibration; R^2C, coefficients of calibration; RMSEP, root mean square error of prediction; R^2P, coefficients of prediction; RMSECV, root mean square error of cross-calibration; RER, Range Error Ratio; RPD, Residual Predictive Performance; SEL, Standard Error of reference method.

Both spectroscopic techniques also accurately predicted the TPC content of brown seaweeds (R^2P= 0.94; RER > 10; RPD > 3). The FC method was used as the reference method, which provides an indirect measurement of total polyphenolic content. The sensitive MIR region of 3700-3400 cm^{-1} (**Figure 3. B2**) corresponds to O-H stretching, which is characteristic of polyphenolic compounds. The

results obtained indicate the potential of NIR and MIR to quantitatively assess the TPC content with R^2 ranging from 0.86 to 0.96 and RER > 9 and > 5 for NIR and MIR based models, respectively. According to **Figure 3. B2**, the region 1800-900 cm^{-1} showed the highest sensitivity to the prediction of TPC. However, it is noteworthy that other functional groups are also described in this region. A similar peak at 1025 cm^{-1} was found to be positively correlated with aNDF and ADF (Figure. 3. B4). Furthermore, the region 3800-2800 cm^{-1}, commonly known as the X-H region due to C-H, CH_2 and O-H fingerprints, was found to be associated with quantitative measurements of the structural fibre components in seaweeds. The RMSEP, which ranged between 1.70 and 1.90, indicated that the difference between the NIR predicted and measured Lignin (sa) values, i.e. using the reference method (SEL= 0.31), was relatively high (**Table 2**). aNDF and ADF were poorly predicted by selecting sensitive MIR regions (R^2 <0.5) compared to the whole spectra (R^2 >0.6) which suggests that basic information of the fibre characteristics of the seaweeds was lost via region selection.

In the current study, the models developed to assess the ash content of seaweeds achieved moderate-quality predictions (R^2: 0.76 – 0.82), but the low RPD (1.5 and 1.2, respectively) suggests that the models may have limited application as a quantitative tool for ash analysis. Although the RC plots (**Figures 3. A1 and B1**) identified several regions correlated with the ash Y variables, region selection had a limited effect on improving the NIR and MIR model outputs (**Table 2**). The prediction of IVTDMD using MIR spectroscopy slightly improved from the whole model to region selection (2200-550 and 3750-3450 cm^{-1}), where R^2P increased from 0.66 to 0.72, and the RMSEP decreased from 15.3 to 13.6, respectively. This indicates that these specific regions were prosperous at enhancing useful molecular information in the spectra, which correlated with the digestibility of the seaweeds.

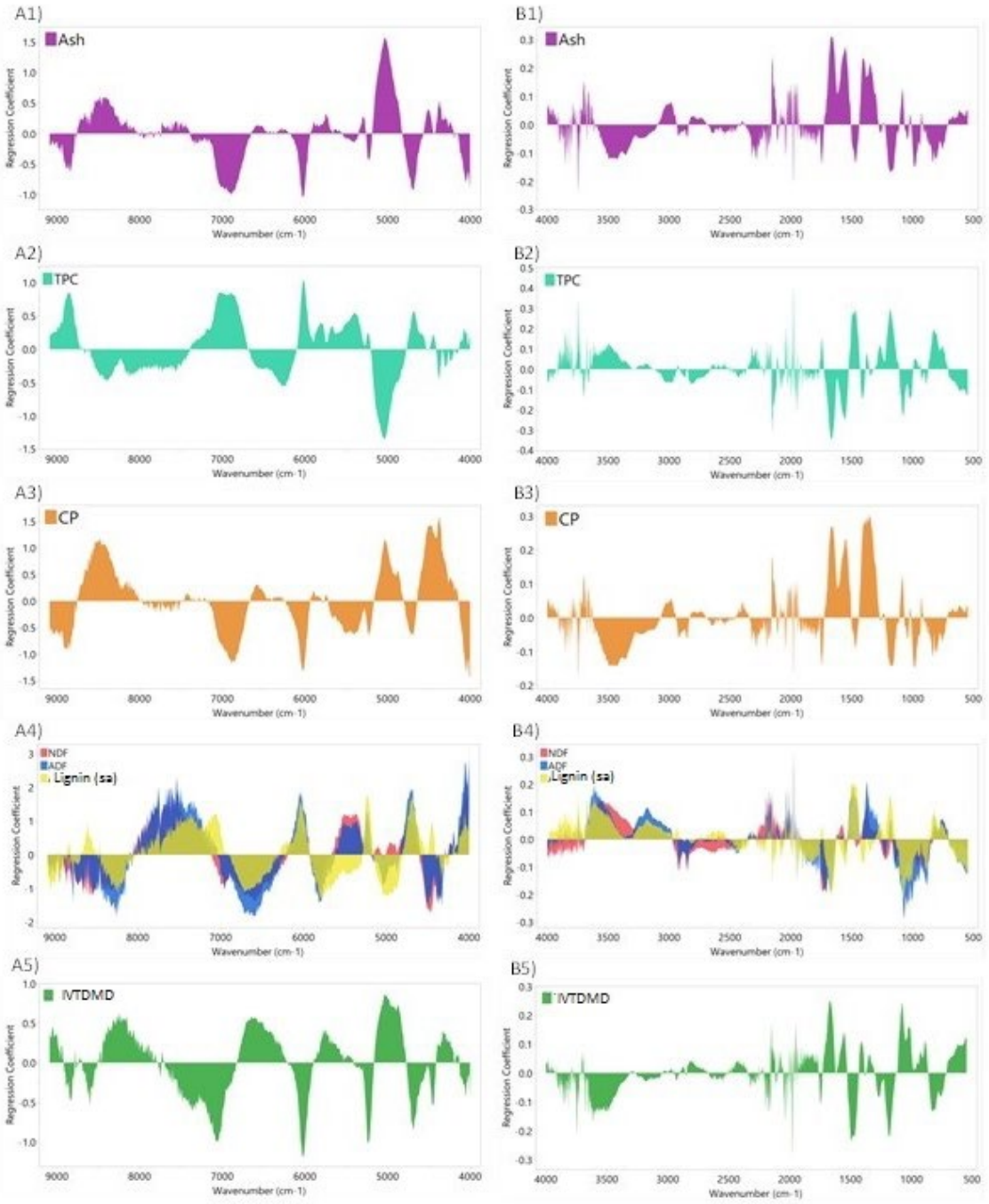

314

315 **Figure 3.** Regression coefficients plots for PLS models based on (A) NIR and (B) MIR spectroscopy, to

316 predict the ash (1), TPC (2), CP (3), Fibre (aNDF/ADF/Lignin (sa)) (4) and IVTDMD (5) of brown

317 seaweeds

318

319

320

4. Discussion

The reference methods descriptive statistics for the calibration and validation data sets showed considerable variability, probably derived from the seasonal- and species-related differences amongst the studied seaweeds. Nevertheless, they were within the normal ranges for brown seaweeds, as reported previously (Makkar et al., 2016; Ometto et al., 2018). With regards to the NIR spectra, the molecular characteristics of the organic constituents of the raw material are often overlapped, which make quantitative estimations problematic (Manley, 2014); however, chemometric techniques can be applied to extract useful information and conduct predictions based on NIR spectral analysis (Stuart, 2012). The peak at 8400-8200 cm^{-1} corresponds with second and third C-H overtone regions, and the 6800-6200 and 5800-5600 cm^{-1} peaks overlap with the first C-H overtone region. The peaks at 5200-5100 cm^{-1} and 5000-4500 cm^{-1} fall within the region associated with C-H and O-H combinations. The latter region was also previously associated with protein bands in wheat samples comprising of N-H bending and C-H/C-O stretching (Manley, 2014).

MIR spectra provide information on fundamental molecular vibrations of the functional groups, which are more specific compared to the harmonic vibrations and overtone absorptions observed in the NIR spectrum. As expected, a large variability was observed in the fingerprint region which represents a heterogeneous group of molecular characteristics (Belanche et al., 2014). Based on the literature, the peak at 1025 cm^{-1} may be assigned to the C-O and C-C stretching vibrations of pyranose rings which are ubiquitous amongst polysaccharides in seaweeds (Pereira et al., 2013). Likewise, this region of the MIR spectra of brown seaweeds has also been attributed to O-H bending of guluronic acid, a copolymer of alginate, the main structural polysaccharide (Sakugawa et al., 2004). The peaks in the MIR spectrum in the region 1660-1550 cm^{-1} have been previously assigned to the molecular characteristics of proteins in terrestrial forages, primarily due to absorption peaks relating to Amide I (C=O stretching vibration) and Amide II (N-H bending vibration) primary protein features.

346 The PLS-R models developed based on the NIR spectroscopy information showed an excellent CP
347 predictive ability, with an RER> 25 and RPD≥ 7. This result is comparable to Foskolos et al. (2015),
348 who found that NIR spectroscopy accurately predicted (R^2P= 0.94-0.99) the CP of a range of
349 feedstuffs (RER = 39; RPD = 7). As expected, the RC plot showed high sensitivity in the protein band,
350 5000-4500 cm^{-1}, corresponding to N-H and C=O stretching, although region selection did not have a
351 significant impact on model outputs. Similarly, Brás et al. (2005) claimed that developing PLS models
352 based on specific NIR regions did not improve the ability of the model to predict the protein content
353 of soybean flour. However, the authors found that excluding the MIR region 2295-1750 cm^{-1}
354 improved prediction efficiency.
355 Regarding TPC, the region 1800-900 cm^{-1} showed the highest sensitivity for the prediction of TPC.
356 This finding was expected due to the contribution of this region to the description of the ring
357 structure of polyphenolic compounds (Ricci et al., 2015). However, it is noteworthy that other
358 functional groups are also described in this region. Previous studies have also found specific regions
359 of the infrared spectrum related to the fibre fractions of various terrestrial forages. In the current
360 study, the MIR regions identified as sensitive to aNDF, ADF and Lignin (sa) were in the ranges 2200-
361 550 and 3800-2800 cm^{-1} which agrees with the findings of Pereira et al. (2013) and Belanche et al.
362 (Belanche et al., 2014). The latter mainly focused their analysis in the 1500-600 cm^{-1} spectral range
363 and attributed the peak at 1032 cm^{-1} to the content of cellulose (C-O stretching). Therefore, the
364 authors concluded that this region was important for the measurement of aNDF. Furthermore, the
365 region 3800-2800 cm^{-1}, commonly known as the X-H region due to C-H, CH_2 and O-H fingerprints,
366 was found to be associated with quantitative measurements of the structural fibre components in
367 seaweeds. Similarly, the region of 8000-6000 cm^{-1} of the NIR spectrum, which corresponds to C-H
368 overtone regions, was associated with the prediction of fibre components. This finding is supported
369 by Obregón-Cano et al. (2019). They also found that C-H and CH_2 groups of structural carbohydrates
370 significantly contributed to the prediction of ADF fractions of Brassicas using NIR spectroscopy,
371 whilst Huang et al. (2011) applied the entire NIR spectrum to quantitatively measure the cellulose,

hemicellulose, and Lignin (sa) contents in rice straw. The NIR model quality for predicting the Lignin (sa) content of brown seaweeds (R^2P of > 0.8 and RPD = 1.9) in this study was comparable to that developed by Huang et al. (2011) (R^2P = 0.78 and RPD = 2.25). Belanche et al. (2014) applied MIR to predict the aNDFom content of various forage-based feeds. The authors employed a larger dataset (n = 150) and achieved slightly more accurate models (RPD = 2.66) compared to the use of MIR models to predict the aNDF content of brown seaweeds in this study (RPD= 1.39). Foskolos et al. (2015) found better NIR performance for predicting the aNDFom content of a more extensive database of various feedstuffs (n= 809) with R^2 ranging from 0.94-0.98 and RER and RPD up to 27 and 6, respectively. In the current study, a relatively smaller dataset was employed (n= 120). These comparisons suggest that a larger dataset would improve the robustness of MIR and NIR model performance for determining the fibre content of brown seaweeds. Although the models achieved a moderate predictive ability, the speed of analysis, minimal preparation, and lower cost are advantageous compared to the reference method. The prediction of ash obtained by NIR in the present study were less accurate than those found by Pojić et al. (2010) in legumes (R^2: 0.89 - 0.97; RPD: 2.7 - 4.2).

Aufrere and Michalet-Doreau (1988) observed that NIR could be used to predict the IVTDMD of forages, which can be used as an indirect predictor of animal performance. However, studies relating to the use of MIR to predict the digestibility of livestock feeds are limited (Shi et al., 2019). The models developed in the present study showed a modest predictive ability, which was improved when specific regions were selected. No apparent reason can be related to this improvement. At this stage, no speculations can be made given the complexity of the biochemical (fibre digestibility, CP digestibility, antinutritional factors) and experimental factors (source of rumen digesta, experimental conditions) which contribute to determining the IVTDMD of ruminant feeds (Yáñez-Ruiz et al., 2016). Lundberg et al. (2004) applied NIR to predict the *in vitro* dry matter digestibility of legume-grass forages, achieving similar results to the current study (R^2P = 0.82 vs > 80, respectively). Overall, the

optimised IVTDMD models showed weak predictive performances; therefore, their use would be limited to qualitative analysis given the low RER (< 4) and RPD (< 1.6) values.

Overall, NIR outperformed the predictive ability of MIR models for most of the tested parameters. This agrees with Shi et al. (2019) and Brás et al. (2005) who found superior predictive modelling using NIR over MIR to estimate the CP of wheat and soybean flour, respectively. Ferreira et al. (2014) determined that NIR and MIR showed comparable abilities to measure soybean quality (protein, lipid and ash content) but identified that NIR could be more applicable for the measurement of protein, whilst MIR was more successful for accurately determining the ash content. A similar comparison could be drawn from the results of the current study. MIR techniques could be used to accurately predict the ash content of brown seaweeds, whilst NIR has a better predictive power for assessing the CP and TPC content. A possible explanation for the superiority of NIR over MIR techniques might be related to differences in the sensitivity of the techniques to sample heterogeneity and particle size (Hell et al., 2016). Advantages might be gained by combining MIR and NIR spectra in PLS-R model development, a technique called "data fusion", which could serve as a potentially more robust method (Brás et al., 2005) compared to single technique approaches explored here. However, this approach must demonstrate a superior predictive accuracy than is achieved with the sum of both techniques when conducted separately, a result which few studies have achieved.

The ultimate objective of the application of infrared spectroscopy techniques is to replace wet analytical methods. However, it needs to be considered that, as a secondary feed analysis method, the accuracy of these techniques is fundamentally dependent on the accuracy of the reference methods. According to the results, and as outlined previously (Manley, 2014), infrared spectroscopy can enable several predictions (protein, fibre, polyphenolic compounds) from a single spectrum, provided that the conditions were the same as when the calibration models were developed. Based on current models, the evaluations of CP and TPC using both infrared spectroscopic techniques were considered to have good prediction capabilities, whilst models for predicting ash, aNDF, ADF, Lignin

(sa) and IVTDMD were less successful. Therefore, the potential to extract nutritional information from a single spectrum, based on these reference methods, has variable predictive ability. Furthermore, when compared to the SEL (i.e. error of the reference method), the root mean square errors of the models were relatively high. Taking into consideration the challenges of conventional laboratory methods, including the limited ability to measure more than one chemical parameter at a time, infrared spectroscopy methods can provide an alternative method which offers real-time, multiple parameter analysis. The development of more globular equations would increase their robustness and precision of the models, but this would require the addition of seaweed samples collected across multiple years and various environments; this would increase the spectral and chemical diversity of the samples compared to those presented in the current study.

5. Conclusions

The calibration and validation statistics obtained in this study clearly showed the potential of infrared spectroscopy techniques to assess the nutritive value of seaweeds. The results illustrate the ability of the regression models to accurately predict the CP content and TPC of brown seaweeds. The models created to measure ash, fibre and IVTDMD showed moderate predictive performance and could be used as a rapid screening tool for qualitative analysis. Further development of the models using larger and more chemically diverse sample datasets would improve model robustness and accuracy. In summary, vibrational spectroscopy-based techniques could be applied to seaweed to rapidly predict the nutritive value of this emerging feed ingredient in the ruminant diet. This should allow stakeholders to integrate these techniques to supplement, but not replace, conventional wet chemistry methods when determining the value of seaweeds as a feed ingredient in ruminant diets.

Funding

This research was funded by Department for Economy (DfE).

Declaration of interests

The authors declare no competing financial interest.

449 **References**

450 Angell, A.R., Mata, L., de Nys, R., Paul, N.A., 2016. The protein content of seaweeds: a universal
451 nitrogen-to-protein conversion factor of five. J. Appl. Phycol. https://doi.org/10.1007/s10811-
452 015-0650-1

453 AOAC, 2000. Official methods of analysis, association of analytical chemists. 15th ed., Washington D.
454 C. Washingt. D. C. USA 141–144. https://doi.org/10.1007/978-3-642-31241-0

455 Aufrere, J., Michalet-Doreau, B., 1988. Comparison of methods for predicting digestibility of feeds.
456 Anim. Feed Sci. Technol. https://doi.org/10.1016/0377-8401(88)90044-2

457 Bai, M., Qin, G., Sun, Z., Long, G., 2016. Relationship between molecular structure characteristics of
458 feed proteins and protein in vitro digestibility and solubility. Asian-Australasian J. Anim. Sci. 29,
459 1159–1165. https://doi.org/10.5713/ajas.15.0701

460 Belanche, A., Weisbjerg, M.R., Allison, G.G., Newbold, C.J., Moorby, J.M., 2014. Measurement of
461 rumen dry matter and neutral detergent fiber degradability of feeds by Fourier-transform
462 infrared spectroscopy. J. Dairy Sci. 97, 2361–2375. https://doi.org/10.3168/jds.2013-7491

463 Belanche, A., Weisbjerg, M.R., Allison, G.G., Newbold, C.J., Moorby, J.M., 2013. Estimation of feed
464 crude protein concentration and rumen degradability by Fourier-transform infrared
465 spectroscopy. J. Dairy Sci. https://doi.org/10.3168/jds.2013-7127

466 Bikker, P., Stokvis, L., van Krimpen, M.M., van Wikselaar, P.G., Cone, J.W., 2020. Evaluation of
467 seaweeds from marine waters in Northwestern Europe for application in animal nutrition.
468 Anim. Feed Sci. Technol. https://doi.org/10.1016/j.anifeedsci.2020.114460

469 Brás, L.P., Bernardino, S.A., Lopes, J.A., Menezes, J.C., 2005. Multiblock PLS as an approach to
470 compare and combine NIR and MIR spectra in calibrations of soybean flour. Chemom. Intell.
471 Lab. Syst. https://doi.org/10.1016/j.chemolab.2004.05.007

472 de Oliveira, G.A., de Castilhos, F., Renard, C.M.G.C., Bureau, S., 2014. Comparison of NIR and MIR
473 spectroscopic methods for determination of individual sugars, organic acids and carotenoids in
474 passion fruit. Food Res. Int. https://doi.org/10.1016/j.foodres.2013.10.051

475 Ellis, D.I., Muhamadali, H., Haughey, S.A., Elliott, C.T., Goodacre, R., 2015. Point-and-shoot: Rapid
476 quantitative detection methods for on-site food fraud analysis-moving out of the laboratory
477 and into the food supply chain. Anal. Methods. https://doi.org/10.1039/c5ay02048d
478 Evans, F.D., Critchley, A.T., 2014. Seaweeds for animal production use. J. Appl. Phycol. 26, 891–899.
479 https://doi.org/10.1007/s10811-013-0162-9
480 Fearn, T., 2002. Assessing Calibrations: SEP, RPD, RER and R 2 . NIR news.
481 https://doi.org/10.1255/nirn.689
482 Ferreira, D.S., Galão, O.F., Pallone, J.A.L., Poppi, R.J., 2014. Comparison and application of near-
483 infrared (NIR) and mid-infrared (MIR) spectroscopy for determination of quality parameters in
484 soybean samples. Food Control. https://doi.org/10.1016/j.foodcont.2013.07.010
485 Foskolos, A., Calsamiglia, S., Chrenková, M., Weisbjerg, M.R., Albanell, E., 2015. Prediction of rumen
486 degradability parameters of a wide range of forages and non-forages by NIRS. Animal.
487 https://doi.org/10.1017/S1751731115000191
488 Gómez-Ordóñez, E., Rupérez, P., 2011. FTIR-ATR spectroscopy as a tool for polysaccharide
489 identification in edible brown and red seaweeds. Food Hydrocoll.
490 https://doi.org/10.1016/j.foodhyd.2011.02.009
491 Haughey, S.A., Galvin-King, P., Malechaux, A., Elliott, C.T., 2015. The use of handheld near-infrared
492 reflectance spectroscopy (NIRS) for the proximate analysis of poultry feed and to detect
493 melamine adulteration of soya bean meal. Anal. Methods.
494 https://doi.org/10.1039/c4ay02470b
495 Hell, J., Prückler, M., Danner, L., Henniges, U., Apprich, S., Rosenau, T., Kneifel, W., Böhmdorfer, S.,
496 2016. A comparison between near-infrared (NIR) and mid-infrared (ATR-FTIR) spectroscopy for
497 the multivariate determination of compositional properties in wheat bran samples. Food
498 Control. https://doi.org/10.1016/j.foodcont.2015.08.003
499 Holden, L.A., 1999. Comparison of methods of in vitro dry matter digestibility for ten feeds. J. Dairy
500 Sci. https://doi.org/10.3168/jds.S0022-0302(99)75409-3

501 Holdt, S.L., Kraan, S., 2011. Bioactive compounds in seaweed: Functional food applications and
502 legislation. J. Appl. Phycol. https://doi.org/10.1007/s10811-010-9632-5
503 Huang, C., Han, L., Liu, X., Ma, L., 2011. The rapid estimation of cellulose, hemicellulose, and lignin
504 contents in rice straw by near infrared spectroscopy. Energy Sources, Part A Recover. Util.
505 Environ. Eff. https://doi.org/10.1080/15567030902937127
506 Li, Y., Fu, X., Duan, D., Liu, X., Xu, J., Gao, X., 2017. Extraction and Identification of Phlorotannins
507 from the Brown Alga, Sargassum fusiforme (Harvey) Setchell. Mar. Drugs.
508 https://doi.org/10.3390/md15020049
509 Lundberg, K.M., Hoffman, P.C., Bauman, L.M., Berzaghi, P., 2004. Prediction of Forage Energy
510 Content by Near Infrared Reflectance Spectroscopy and Summative Equations. Prof. Anim. Sci.
511 https://doi.org/10.15232/S1080-7446(15)31309-7
512 Maia, M.R.G., Fonseca, A.J.M., Cortez, P.P., Cabrita, A.R.J., 2019. In vitro evaluation of macroalgae as
513 unconventional ingredients in ruminant animal feeds. Algal Res.
514 https://doi.org/10.1016/j.algal.2019.101481
515 Makkar, H.P.S., Tran, G., Heuzé, V., Giger-Reverdin, S., Lessire, M., Lebas, F., Ankers, P., 2016.
516 Seaweeds for livestock diets: A review. Anim. Feed Sci. Technol. 212, 1–17.
517 https://doi.org/10.1016/j.anifeedsci.2015.09.018
518 Manley, M., 2014. Near-infrared spectroscopy and hyperspectral imaging: Non-destructive analysis
519 of biological materials. Chem. Soc. Rev. https://doi.org/10.1039/c4cs00062e
520 Martens, H., Naes, T., 1989. Assesment, validation and choice of calibration method., in: Multivariate
521 Calibration.
522 McDonald, P., Edwards, R. a, Greenhalgh, J.F.D., Morgan, C. a, Sinclair, L. a, Wilkinson, R.G., 2011.
523 Animal nutrition 7th Edition, Prentice Hall.
524 Molina-Alcaide, E., Carro, M.D., Roleda, M.Y., Weisbjerg, M.R., Lind, V., Novoa-Garrido, M., 2017. In
525 vitro ruminal fermentation and methane production of different seaweed species. Anim. Feed
526 Sci. Technol. https://doi.org/10.1016/j.anifeedsci.2017.03.012

527 Obregón-Cano, S., Moreno-Rojas, R., Jurado-Millán, A.M., Cartea-González, M.E., De Haro-Bailón, A.,
528 2019. Analysis of the acid detergent fibre content in turnip greens and turnip tops (Brassica
529 rapa L. SubSp. Rapa) by means of near-infrared reflectance. Foods 8.
530 https://doi.org/10.3390/foods8090364
531 Ometto, F., Steinhovden, K.B., Kuci, H., Lunnbäck, J., Berg, A., Karlsson, A., Handå, A., Wollan, H.,
532 Ejlertsson, J., 2018. Seasonal variation of elements composition and biomethane in brown
533 macroalgae. Biomass and Bioenergy. https://doi.org/10.1016/j.biombioe.2017.11.006
534 Pereira, L., Gheda, S.F., Ribeiro-Claro, P.J.A., 2013. Analysis by Vibrational Spectroscopy of Seaweed
535 Polysaccharides with Potential Use in Food, Pharmaceutical, and Cosmetic Industries. Int. J.
536 Carbohydr. Chem. https://doi.org/10.1155/2013/537202
537 Pojić, M., Mastilović, J., Palić, D., Pestorić, M., 2010. The development of near-infrared spectroscopy
538 (NIRS) calibration for prediction of ash content in legumes on the basis of two different
539 reference methods. Food Chem. https://doi.org/10.1016/j.foodchem.2010.05.013
540 Ricci, A., Olejar, K.J., Parpinello, G.P., Kilmartin, P.A., Versari, A., 2015. Application of Fourier
541 transform infrared (FTIR) spectroscopy in the characterisation of tannins. Appl. Spectrosc. Rev.
542 50, 407–442. https://doi.org/10.1080/05704928.2014.1000461
543 Robertson, J.B., Van Soest, P.J., 1981. The detergent system of analysis and its application to human
544 foods, in: The Analysis of Dietary Fiber in Food.
545 Sakugawa, K., Ikeda, A., Takemura, A., Ono, H., 2004. Simplified method for estimation of
546 composition of alginates by FTIR. J. Appl. Polym. Sci. https://doi.org/10.1002/app.20589
547 Shenk, J.S., Westerhaus, M.O., 1991. Population Definition, Sample Selection, and Calibration
548 Procedures for Near Infrared Reflectance Spectroscopy. Crop Sci.
549 https://doi.org/10.2135/cropsci1991.0011183x003100020049x
550 Shi, H., Lei, Y., Louzada Prates, L., Yu, P., 2019. Evaluation of near-infrared (NIR) and Fourier
551 transform mid-infrared (ATR-FT/MIR) spectroscopy techniques combined with chemometrics
552 for the determination of crude protein and intestinal protein digestibility of wheat. Food Chem.

272, 507–513. https://doi.org/10.1016/j.foodchem.2018.08.075

Stuart, B.H., 2012. Infrared Spectroscopy of Biological Applications: An Overview, in: Encyclopedia of Analytical Chemistry. https://doi.org/10.1002/9780470027318.a0208.pub2

Theodoridou, K., Yu, P., 2013. Application potential of ATR-FT/IR molecular spectroscopy in animal nutrition: Revelation of protein molecular structures of canola meal and presscake, as affected by heat-processing methods, in relationship with their protein digestive behavior and utili. J. Agric. Food Chem. 61, 5449–5458. https://doi.org/10.1021/jf400301y

Van Soest, P.J., Robertson, J.B., Lewis, B.A., 1991. Methods for Dietary Fiber, Neutral Detergent Fiber, and Nonstarch Polysaccharides in Relation to Animal Nutrition. J. Dairy Sci. https://doi.org/10.3168/jds.S0022-0302(91)78551-2

Wang, Y., McAllister, T.A., 2011. Brown algae as a feed additive: Nutritional and health impacts on ruminants - A review. S.R. Borgearo (Ed.), Animal feed: types, nutrition, and safety, Nova Science Publishers (2011), pp. 1-32

Williams, P., 2004. Near-Infrared technology: Getting the best out of light, Near Infrared Technology.

Yáñez-Ruiz, D.R., Bannink, A., Dijkstra, J., Kebreab, E., Morgavi, D.P., O'Kiely, P., Reynolds, C.K., Schwarm, A., Shingfield, K.J., Yu, Z., Hristov, A.N., 2016. Design, implementation and interpretation of in vitro batch culture experiments to assess enteric methane mitigation in ruminants-a review. Anim. Feed Sci. Technol. https://doi.org/10.1016/j.anifeedsci.2016.03.016

Supplementary material

Table S.1. Optimisation of pre-processing treatments during PLS-R model development. Optimal pre-treatments are shown in bold.

		NIR						MIR					
Chemical parameter	**Pre-processing**	**LV**	**RMSEC**	**R^2C**	**RMSEP**	**R^2P**	**RMSECV**	**LV**	**RMSEC**	**R^2C**	**RMSEP**	**R^2P**	**RMSECV**
Ash:	Raw spectra	5	5.25	0.68	4.36	0.85	5.64	3	5.12	0.76	4.74	0.74	5.60
	SNV	3	5.24	0.68	4.42	0.85	5.60	4	4.99	0.77	4.19	0.82	5.54
	FD	4	4.97	0.72	4.58	0.83	5.43	3	5.32	0.73	4.75	0.75	7.17
	SD	**5**	**4.36**	**0.79**	**5.03**	**0.79**	**5.08**	2	5.49	0.71	5.37	0.68	6.43
	SNV + FD	4	4.96	0.72	4.57	0.83	5.55	4	4.78	0.79	4.22	0.81	5.65
	SNV + SD	4	4.55	0.77	5.04	0.79	5.24	3	4.55	0.81	4.87	0.74	6.14
	SNV + FD + SG	4	4.97	0.72	4.58	0.83	5.56	**4**	**4.83**	**0.79**	**4.18**	**0.82**	**5.65**
	SNV + SD + SG	4	4.78	0.74	4.78	0.81	5.26	4	4.79	0.79	4.16	0.82	5.91
TPC:	Raw spectra	10	0.19	0.95	0.24	0.93	0.23	5	0.29	0.89	0.29	0.87	0.34
	SNV	9	0.17	0.96	0.22	0.94	0.21	7	0.22	0.94	0.22	0.93	0.27
	FD	7	0.20	0.94	0.25	0.93	0.24	8	0.15	0.97	0.31	0.86	0.30
	SD	6	0.18	0.96	0.26	0.92	0.25	5	0.22	0.94	0.35	0.82	0.34
	SNV + FD	**9**	**0.15**	**0.97**	**0.21**	**0.95**	**0.21**	5	0.20	0.95	0.27	0.89	0.26
	SNV + SD	7	0.14	0.97	0.23	0.94	0.24	**6**	**0.19**	**0.95**	**0.23**	**0.92**	**0.31**
	SNV + FD + SG	9	0.16	0.97	0.21	0.95	0.21	5	0.20	0.95	0.27	0.89	0.26
	SNV + SD + SG	7	0.17	0.96	0.23	0.94	0.23	6	0.18	0.96	0.28	0.88	0.26
CP:	Raw spectra	10	0.55	0.99	0.75	0.99	0.74	3	1.47	0.93	2.03	0.85	1.58
	SNV	10	0.50	0.99	0.58	0.99	0.65	**6**	**1.11**	**0.96**	**1.11**	**0.96**	**1.27**
	FD	**10**	**0.43**	**0.99**	**0.51**	**0.99**	**0.65**	8	0.83	0.98	1.53	0.92	1.56
	SD	9	0.38	0.99	0.74	0.99	0.91	9	0.40	0.99	1.87	0.89	1.87
	SNV + FD	8	0.56	0.99	0.77	0.99	0.76	9	0.37	0.99	0.99	0.97	1.08
	SNV + SD	8	0.53	0.99	0.92	0.98	1.11	10	0.27	0.99	1.49	0.92	1.73
	SNV + FD + SG	8	0.56	0.99	0.77	0.99	0.75	10	0.36	0.99	0.99	0.97	1.10
	SNV + SD + SG	8	0.70	0.98	0.88	0.98	0.91	10	0.38	0.99	1.23	0.95	1.27
aNDF:	Raw spectra	10	4.38	0.86	6.79	0.71	5.96	4	7.07	0.52	7.77	0.63	7.66
	SNV	6	5.40	0.77	7.85	0.57	6.08	5	6.22	0.66	7.36	0.66	7.33
	FD	10	3.94	0.89	6.27	0.76	5.55	5	5.71	0.72	7.90	0.58	7.45
	SD	**9**	**2.55**	**0.95**	**5.58**	**0.82**	**6.50**	1	7.91	0.29	8.93	0.52	8.63
	SNV + FD	8	4.59	0.84	6.48	0.73	5.85	4	5.23	0.77	7.45	0.64	7.29
	SNV + SD	5	4.58	0.84	7.02	0.66	6.68	3	5.89	0.70	8.49	0.48	8.60
	SNV + FD + SG	8	4.62	0.84	6.50	0.73	5.85	4	5.27	0.77	7.45	0.64	7.21
	SNV + SD + SG	6	5.24	0.79	5.97	0.77	6.31	**8**	**3.08**	**0.93**	**7.01**	**0.72**	**7.07**
ADF:	Raw spectra	10	1.56	0.86	2.37	0.74	2.02	4	2.84	0.55	2.54	0.40	3.15
	SNV	8	1.67	0.83	2.39	0.73	2.04	5	2.45	0.69	2.38	0.55	2.90
	FD	9	1.31	0.90	1.88	0.84	1.81	9	1.15	0.94	2.82	0.50	2.62
	SD	7	1.09	0.93	1.70	0.89	2.30	5	1.82	0.85	2.79	0.18	3.28
	SNV + FD	8	1.44	0.88	1.75	0.86	1.86	8	1.15	0.94	2.45	0.56	2.31
	SNV + SD	**7**	**1.07**	**0.94**	**1.87**	**0.86**	**2.21**	3	2.45	0.69	3.04	0.04	3.12
	SNV + FD + SG	8	1.44	0.88	1.74	0.86	1.85	**9**	**1.04**	**0.95**	**2.29**	**0.64**	**2.25**
	SNV + SD + SG	5	1.70	0.83	1.88	0.85	2.09	8	1.15	0.94	2.28	0.57	2.53
Lignin (sa):	Raw spectra	9	1.52	0.89	1.83	0.86	1.81	3	2.35	0.72	2.23	0.78	2.60
	SNV	7	1.55	0.88	1.89	0.85	1.76	7	1.60	0.88	1.68	0.88	2.10
	FD	7	1.48	0.89	1.70	0.88	1.83	10	0.80	0.97	1.92	0.84	2.33
	SD	4	1.61	0.87	1.89	0.85	1.88	2	2.58	0.64	2.68	0.61	2.96
	SNV + FD	4	1.67	0.86	1.84	0.86	1.86	**8**	**0.92**	**0.96**	**1.79**	**0.86**	**1.87**
	SNV + SD	**5**	**1.46**	**0.90**	**1.90**	**0.85**	**1.89**	7	0.88	0.97	1.87	0.84	2.49
	SNV + FD + SG	4	1.67	0.86	1.84	0.86	1.86	8	0.96	0.96	1.82	0.85	1.86
	SNV + SD + SG	4	1.66	0.86	1.87	0.86	1.85	8	0.91	0.96	1.62	0.88	2.10
IVTDMD:	Raw spectra	6	9.39	0.85	11.80	0.81	10.30	5	10.50	0.80	15.80	0.61	11.74
	SNV	5	9.28	0.85	12.10	0.80	10.10	3	9.33	0.85	14.40	0.68	10.00
	FD	4	9.25	0.85	11.80	0.81	10.10	4	10.70	0.79	15.00	0.65	12.27
	SD	**4**	**8.65**	**0.87**	**11.70**	**0.81**	**9.68**	2	12.20	0.72	16.70	0.54	13.91
	SNV + FD	2	9.75	0.83	12.60	0.78	10.40	3	9.42	0.84	13.60	0.72	10.35
	SNV + SD	4	8.59	0.87	12.10	0.80	10.10	5	7.71	0.90	14.00	0.70	11.67
	SNV + FD + SG	2	9.76	0.83	12.60	0.78	10.40	**7**	**5.73**	**0.95**	**15.30**	**0.66**	**9.52**
	SNV + SD + SG	3	0.83	0.85	11.80	0.81	10.20	3	9.96	0.82	14.00	0.70	10.94

SNV, standard normal variate; FD, first derivative; SD, second derivative; SG, Savitzky–Golay smoothing; LV, Latent Variables; RMSEC, root mean square error of calibration; R^2C, coefficients of calibration; RMSEP, root mean square error of prediction; R^2P, coefficients of prediction; RMSECV, root mean square error of cross-calibration